Dielectric properties of $(Bi_{0.9}La_{0.1})_2NiMnO_6$ thin films: Determining the intrinsic electric and magnetoelectric response

E. Langenberg,[1,3,*] I. Fina,[2] J. Ventura,[1] B. Noheda,[4] M. Varela,[1] and J. Fontcuberta[2]

[1]*Departament de Física Aplicada i Òptica, Universitat de Barcelona, Martí i Franquès 1, 08028 Barcelona, Spain*

[2]*Institut de Ciència de Materials de Barcelona, CSIC, Campus de la UAB, 08193 Bellaterra, Spain*

[3]*Instituto de Nanociencia de Aragón, Universidad de Zaragoza, Mariano Esquillor, 50018 Zaragoza, Spain*

[4]*Zernike Institute for Advanced Materials, University of Groningen, Groningen 9747AG, the Netherlands*

(Received 23 May 2012; published 8 August 2012)

We have used temperature-dependent impedance spectroscopy to study the dielectric response of thin films of ferromagnetic and ferroelectric $(Bi_{0.9}La_{0.1})_2NiMnO_6$ oxide. This technique has allowed us to disentangle its intrinsic dielectric response and extract the dielectric permittivity of ∼220, which is in close agreement with bulk values but significantly smaller than early reported values for similar thin films. The permittivity is found to be temperature independent in the vicinity of the ferromagnetic transition temperature and independent of magnetic field. We have shown that the measured magnetocapacitance arises from the magnetoresistance of the films, thus indicating a negligible magnetoelectric coupling in these double perovskites, probably due to the different energy scales and mechanisms of ferroelectric and magnetic order.

DOI: 10.1103/PhysRevB.86.085108 PACS number(s): 75.85.+t, 77.22.−d, 73.40.−c, 73.61.−r

I. INTRODUCTION

The possibility of controlling the magnetization or polarization by an electric or magnetic field, respectively, in materials displaying ferroelectric and magnetic order in the same phase, so-called multiferroic materials, has triggered a great amount of research.[1] The coupling between these two ferroic orders not only is interesting in terms of fundamental research but also could have great technological impact in some applications, i.e., spintronics. For this latter purpose, ferromagnetic multiferroics would have greater advantages over antiferromagnetic multiferroics, because the net magnetization could allow easier control of the magnetic state and subsequently its polar state in the presence of large magnetoelectric coupling. However, the antiferromagnetic order prevails in multiferroic perovskite oxides; thus, research should focus on identification of new ferromagnetic ferroelectrics.

The scarcity of ferromagnetic multiferroics might be overcome by designing oxides with double-perovskite structure, $A_2BB'O_6$, because the combination of cations with different electronic configurations at the B-site enables engineering superexchange ferromagnetic paths by appropriately choosing the B–B′ cations.[2] In the case of Bi_2NiMnO_6 (BNMO) and La_2NiMnO_6 (LNMO), both compounds are ferromagnetic below $T_{FM} \approx 140$ and 280 K, respectively,[3,4] but only the former is ferroelectric ($T_{FE} \approx 485$ K).[3] The magnetoelectric coupling might be favored in the solid solution BNMO–LNMO due to the approach of the two transition temperatures (T_{FM}, T_{FE}),[5] because La-doping in BNMO diminishes the ferroelectric response while it increases the magnetic Curie temperature.[6] It has been shown that in bulk form,[6] up to 20% of La-doping, the structure of $(Bi_{1-x}La_x)_2NiMnO_6$ remains noncentrosymmetric monoclinic C2, for which ferroelectric order would be permitted. Recently, we have shown that $(Bi_{0.9}La_{0.1})_2NiMnO_6$ (BLNMO) thin films are ferroelectric, having a $T_{FE} \approx 450$[7], and ferromagnetic below 100 K,[8] which bears out the multiferroic character of the material.

Directly stating the coupling between the two ferroic properties entails measuring the effect of the electric field on the magnetization or, equivalently, the effect of the magnetic field on the electric polarization. Yet many multiferroic materials tend to be poor insulators, preventing a sufficient electric field from being applied[9,10] and thus hampering experimental determination of the magnetoelectric coupling. An alternative route to investigating the magnetoelectric character consists of studying the effect on the dielectric permittivity ε of changes of the magnetic state of the magnetic layer—either by applying a magnetic field, the so-called magnetocapacitance, or by searching for variations of ε in the temperature dependence $\varepsilon(T)$ in the vicinity of the magnetic transition temperature.[11]

However, determining the intrinsic dielectric permittivity, and therefore the real dielectric response of multiferroics, can be, by itself, an arduous task. First, it is well known that extrinsic contributions, such as parasite capacitances formed at the interface between the dielectric film and the electrodes or at the grain boundaries in ceramic samples, often account for the apparent colossal dielectric constants reported for many dielectric materials.[12–17] Second, the leaky behavior of most multiferroic materials may give rise to an apparent large magnetodielectric response, when in reality it might not be the permittivity but the resistivity of the dielectric material that is changing either on applying a magnetic field or with temperature.[9] Whereas the former contribution can in principle be handled by appropriate experimental methods, the role of the latter, which can be of the highest relevance in double-perovskite thin films due to the multivalent configuration of B-cations, is still to be addressed.

These difficulties become apparent when comparing dielectric data reported for double-perovskite thin films. For instance, it has been reported that LNMO films show temperature (T) dependence and frequency (ν) dependence of the dielectric permittivity $\varepsilon(T,\nu)$,[18] which was attributed to temperature-dependent electric dipole relaxation. Similar $\varepsilon(T,\nu)$ features have been reported for BNMO films,[19] where a modest value ($\varepsilon \approx 50$) was reported at low temperature and an unexpected sharp increase takes place at 150 K ($\varepsilon \approx 450$). In contrast, in bulk BNMO, dielectric permittivity was found

to be roughly constant ($\varepsilon \approx 200$) for temperatures well below T_{FE}.[3]

Here, we report on a quantitative study of the apparent temperature-dependent dielectric relaxation of BLNMO thin films, which we prove is driven by the temperature dependence of the resistivity instead of the dielectric relaxation of electric dipoles. Impedance spectroscopy methods[10,12,20] have been used to disentangle extrinsic contributions to the measured permittivity and to extract the temperature dependence of the intrinsic dielectric and resistive properties of $(Bi_{0.9}La_{0.1})_2NiMnO_6$ films. Moreover, we show that the magnetocapacitance of $(Bi_{0.9}La_{0.1})_2NiMnO_6$ films is likely due to extrinsic effects, suggesting a weak intrinsic magnetoelectric coupling in $(Bi,La)_2NiMnO_6$ compounds.

II. EXPERIMENTAL DETAILS

We grew 100-nm-thick BLNMO thin films by pulsed laser deposition on conducting 0.5% Nb-doped $SrTiO_3$ (001) (Nb:STO) substrates. The growth conditions to obtain single-phase samples are reported elsewhere.[21] Sputtered Pt top electrodes were deposited through a shadow mask. Dielectric measurements were performed in a probe station, using a top-to-top electrode configuration[22] in the 10–300 K temperature range. An impedance analyzer was used with an applied alternating current (ac) of 50 mV of amplitude operating between 40 Hz and 1 MHz. Magnetocapacitance measurements, varying the magnetic field up to 9 T, were performed in a physical properties measurement system.

III. RESULTS AND DISCUSSION

A. Complex dielectric constant and ac conductivity: Qualitative analysis

Fig. 1 depicts the temperature dependence of the dielectric permittivity at different frequencies, assuming that the measured capacitance C is only due to the dielectric response of the BLNMO film: $C = \varepsilon' \varepsilon_0 A/(2d)$,[22] where A and d are the area of the electrode and the thickness of the film, respectively,

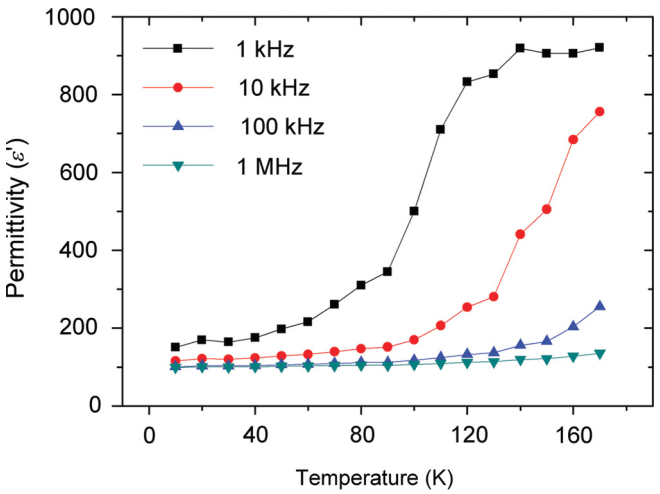

FIG. 1. (Color online) Temperature dependence of the dielectric permittivity of Pt/BLNMO/Nb:STO capacitors measured at different frequencies.

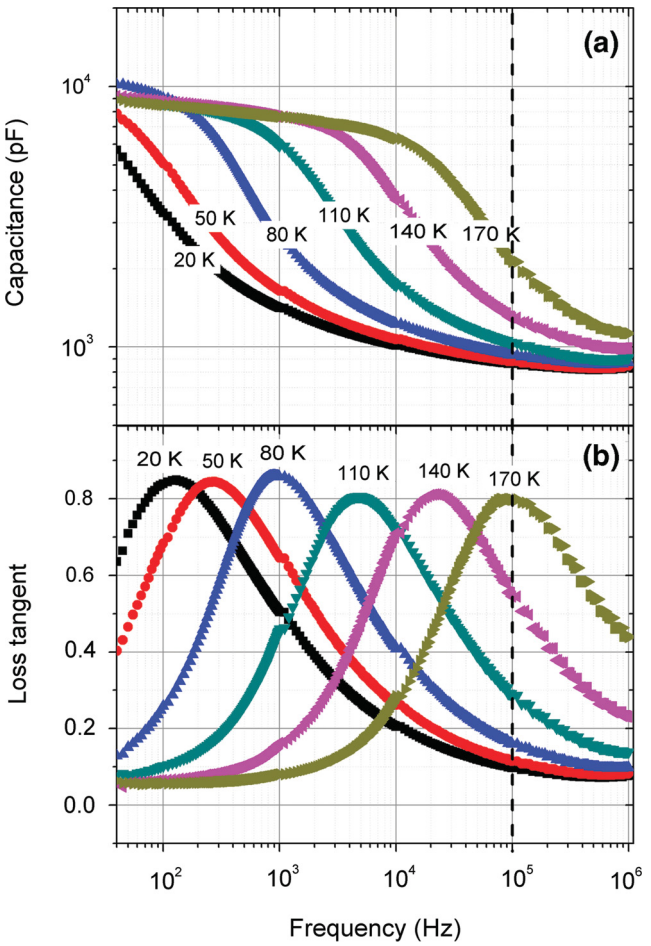

FIG. 2. (Color online) Frequency dependence of (a) the effective capacitance and (b) the loss tangent of Pt/BLNMO/Nb:STO capacitors measured at different temperatures. The dashed line signals the frequency at which magnetocapacitance measurements are done.

and ε_0 and ε' are the vacuum permittivity and the real part of the complex dielectric constant, respectively. The dielectric permittivity ε' increases as temperature rises, with a visible steplike behavior. The steplike feature moves toward higher temperatures on increasing frequency; a similar observation was reported for LNMO thin films.[18] The reported dielectric permittivity of BNMO thin films measured at 100 kHz and at 1 MHz of Refs. 19 and 23 shows a clear resemblance to data in Fig. 1 for 100 kHz and 1 MHz, respectively. Nonetheless, ε' at high temperatures is clearly frequency dependent, and it strongly reduces when frequency is increased. This suggests that extrinsic effects are contributing to the dielectric response,[12,13,15–17] thus claiming a new regard for data and related conclusions.

To assess the frequency response, the complex representation of the dielectric constant $\varepsilon^* = \varepsilon' - i\varepsilon''$ is used. Fig. 2 depicts the frequency dependence of the effective capacitance $C = \varepsilon' \varepsilon_0 A/(2d)$ and the loss tangent $\tan \delta = \varepsilon''/\varepsilon'$ of Pt/BLNMO/Nb:STO capacitors at different temperatures. The measured capacitance [Fig. 2(a)] shows the existence of two frequency regimes, where $C(\nu)$—and thus the permittivity $\varepsilon'(\nu)$—is rather constant, separated by a steplike region accompanied by a peak of $\tan \delta$ and thus the imaginary part

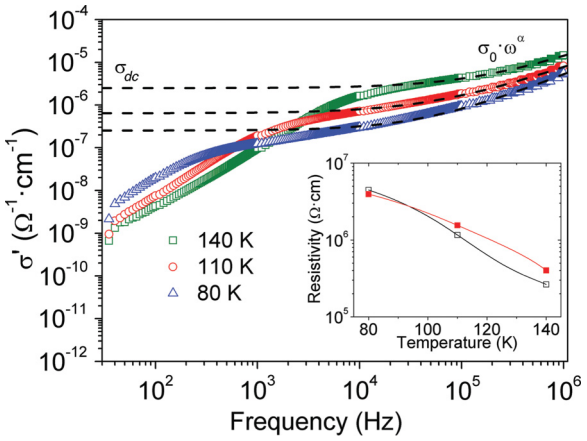

FIG. 3. (Color online) Frequency dependence of σ' at different temperatures. The dashed line indicates the ideal behavior, $\sigma' = \sigma_{dc} + \sigma_0\omega^{\alpha}$ (see text). The inset shows the temperature dependence of the resistivity obtained by extrapolation to zero frequency of σ' from the main panel (solid squares) and by impedance spectroscopy (open squares). Solid lines are visual guides.

of the dielectric constant ε'' [Fig. 2(b)]. Both the steplike region in $C'(\nu)$ and the peak of tan δ (ν) shift toward higher frequencies on increasing temperature. At first sight, this behavior could be attributed to thermally activated Debye-like dielectric relaxation dominating the frequency dependence of $\varepsilon'(\nu)$. The low-frequency dielectric permittivity, obtained assuming that the dielectric response is due to a unique capacitor $\varepsilon' = C \cdot (2d/\varepsilon_0 A)$, is anomalously high ($\varepsilon' \approx 1000$), as shown in Fig. 1, and strongly dependent on temperature. In contrast, at higher frequency, the capacitance is about one order of magnitude smaller and tends to be weakly dependent on frequency, thus signaling a more plausible intrinsic character. The corresponding permittivity is found to be in the range of that reported for BNMO bulk materials.[3]

In the high-frequency range, we can also observe a small but perceptible $\varepsilon'(\nu)$ dependence [Fig. 2(a)], which is at odds with the response of an ideal dielectric, but it is commonly observed in most dielectrics and attributed to the frequency-dependent ac conductivity σ_{ac}. This can be better seen in Fig. 3, where we plot the frequency dependence of the real part (σ') of the complex conductivity ($\sigma^* = i\omega\varepsilon_0\varepsilon^*$, where ω stands for the angular frequency $2\pi\nu$) at various temperatures (80, 110, and 140 K). σ' should be the sum of the frequency-independent direct current (dc) conductivity σ_{dc}, which is always present due to the leakage of the dielectric, and a frequency-dependent term σ_{ac}, which typically shows a power-law dependence on frequency (universal dielectric response contribution): $\sigma_{ac} = \sigma_0\omega^{\alpha}$, $\alpha \leqslant 1$.[13,24] The $\sigma'(\nu)$ log–log data in Fig. 3 show that at high frequency, there is a powerlike $\sigma_{ac}(\nu)$ contribution superimposed to σ_{dc} term responsible for the flattening of $\sigma'(\nu)$ at intermediate frequencies. The extrapolation of $\sigma'(\nu)$ from the plateau toward zero frequency (dashed lines in Fig. 3) allows us to estimate the σ_{dc} of the material or, equivalently, the resistivity at any temperature. Some illustrative values are shown in Fig. 3 (inset; solid squares), where a rough exponential increase of resistance when lowering temperature can be appreciated. When further lowering ν, conductivity is steeply reduced, deviating from the ideal behavior marked in dashed lines. As shown by the data in Fig. 3, this drop is also temperature dependent and shifts toward higher frequencies as temperature rises. Not surprisingly, it coincides with large enhancement of the dielectric constant shown in Fig. 2(a) and the peak of ε'' [Fig. 2(b)].

Next we show that both the low-frequency region and the steplike region are not intrinsic properties of the BLNMO film but rather result from the contribution of interface effects. To obtain more quantitative insight into the dielectric response of the sample, to investigate the number of electrical responses present, and to determine the intrinsic properties of the film, complex impedance ($Z^* = Z' + iZ''$) spectroscopy was performed as described in the following.

B. Impedance spectroscopy: Quantitative analysis

The impedance of the dielectric film can be represented by two circuit elements connected in parallel: one resistive, R, accounting for the leakage of the material, and one capacitive, C, accounting for the dielectric character. Moreover, to account for the nonideal dielectric response attributed to the frequency-dependent ac conductivity (Fig. 3), C is commonly replaced by a constant phase element (CPE).[10,25–27] The impedance of this R-CPE circuit is given by

$$Z^*_{R-\mathrm{CPE}} = \frac{R}{1 + RQ(i\omega)^{\alpha}} \tag{1}$$

where Q and α ($\alpha \leqslant 1$, being $\alpha = 1$ for an ideal capacitor) denote the amplitude and the phase of the CPE, respectively.[10,25–28] Capacitance values, C, can be obtained according to the relationship $C = (Q \cdot R)^{(1/\alpha)}/R$.[28]

A useful representation of impedance data consists of plotting the negative imaginary term of the complex impedance $-Z''$ versus the real term Z'. In this complex impedance plane, the impedance of a dielectric film should depict a semicircle of radius $R/2$ with a maximum at a frequency in which the condition $\omega_{\max} = 1/RC$ is fulfilled, C being the capacitance of an ideal capacitor.[10,12,20,25] In R-CPE elements, the semicircle is slightly depressed, depending on how α deviates from the unity.[10] In Fig. 4(a), we show the illustrative $-Z''$–Z' plot of the impedance measured at 110 K. Data signal the existence of two incomplete semicircles (marked with a dashed line as a visual guide) at high and low frequency, respectively. The existence of these circles indicates that a unique R-CPE element is not sufficient to describe the impedance data, confirming that the dielectric response shown in Sec. III A is not due to the intrinsic dielectric properties of BLNMO thin films alone. Hence, another element should be considered when accounting for the extrinsic contribution, i.e., the resistance of connecting circuit and the interface capacitance, as indicated in the circuit model shown in the inset of Fig. 4(a). Consequently, the impedance of the Pt/BLNMO/Nb:STO system (film + extrinsic contribution) is given by

$$Z^*(R-CPE, R_{\mathrm{ext}} - C_{\mathrm{ext}}) = \frac{R}{1 + R \cdot Q \cdot (i\omega)^{\alpha}} + \frac{R_{\mathrm{ext}}}{1 + i\omega \cdot R_{\mathrm{ext}} \cdot C_{\mathrm{ext}}} \tag{2}$$

where the first and the second terms correspond to the film and the extrinsic contributions, respectively.

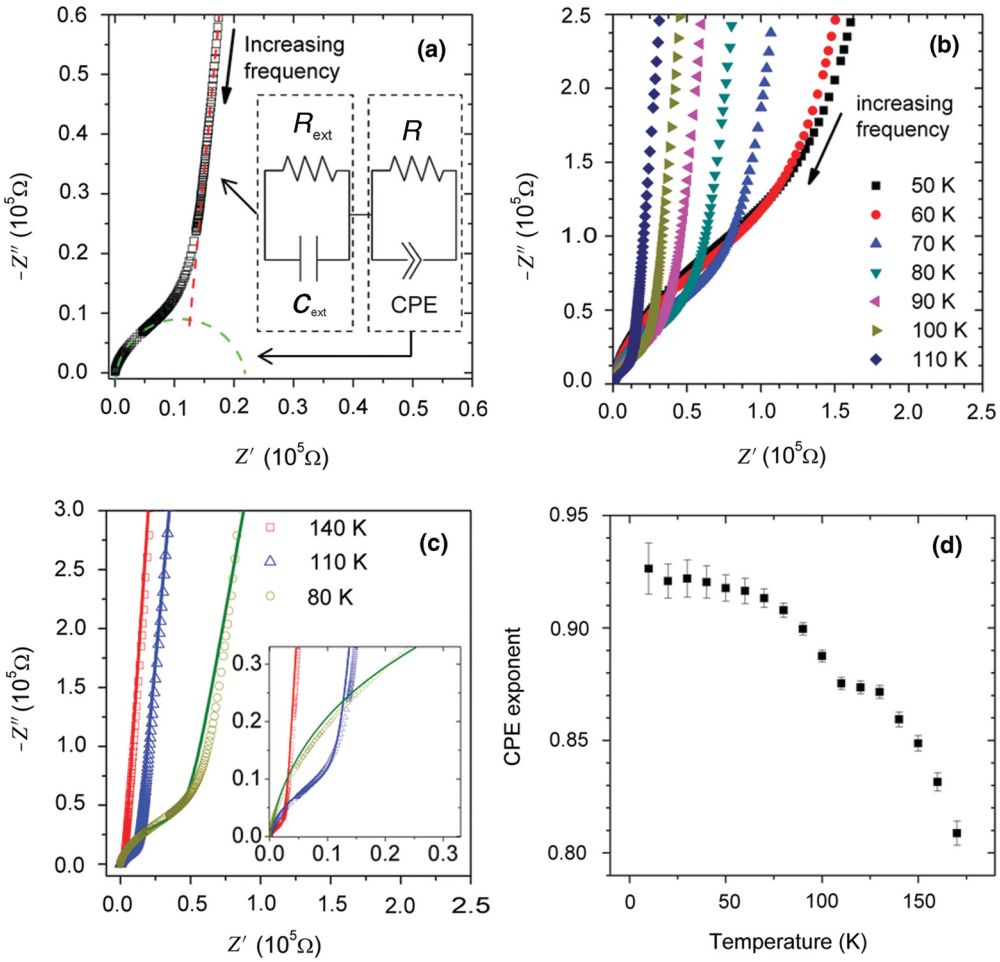

FIG. 4. (Color online) (a) Impedance complex plane ($-Z''$–Z' plots) data at 110 K. The visual guide of the dashed line indicates the two semicircles at high and low frequency. The inset sketch shows the equivalent circuit, describing the different electrical responses present in Pt/BLNMO/Nb:STO capacitors (see text for symbols). (b) $-Z''$–Z' data plots at different temperatures. (c) Experimental data (open symbols) and fitting (solid line) using the model of Eq. (2) of some illustrative temperatures. The inset zooms in on the high-frequency region. (d) Temperature dependence of the CPE exponent.

It can be appreciated in Fig. 4(a) that the radius of the low-frequency semicircle is much larger than that of the high-frequency one; this reflects that the low-frequency contribution is more resistive than the high-frequency contribution. Inspection of the impedance data at different temperatures, shown in Fig. 4(b), indicates that the high-frequency semicircle significantly decreases on increasing temperature, evidencing that the resistivity of the high-frequency contribution decreases as temperature rises, according to data of the conductivity shown in Fig. 3.

Equation (2) was used to fit impedance data to validate the proposed model. In Fig. 4(c), we show some illustrative results of the fits to $-Z''$–Z' data at different temperatures. As shown, model (solid lines) and data match reasonably, which is extended for the rest of the temperatures (not shown) up to 170 K, corroborated by the low goodness-of-fit indicator χ^2 which, in all temperature ranges, is $\sim 10^{-3}$. Above this temperature, the low-frequency contribution nearly dominates the experimentally available frequency range (up to 1 MHz), and accurate extraction of the intrinsic properties (high-frequency contribution) was unfeasible.

Thus, the dielectric behavior shown in Sec. III A can be explained by the formation of a capacitive layer at the interface and by the temperature dependence of the resistivity of the core of the film. The band bending caused by the difference between the work function of the metal and the electronic affinity of the dielectric gives rise to a charge depletion/accumulation region at the interface,[9,10,13,15] which forms a relatively thin layer, behaving as a highly resistive barrier [modeled as a capacitor C_{ext} and a low conductance R_{ext}^{-1} connected in parallel, as illustrated by the circuit model sketched in Fig. 4(a)]. At high frequency, charge carriers have no time to follow the alternating electric field, and the measured capacitance is the film and the interface capacitances in series. However, at low frequencies, charge carriers do respond to the electric field in the low resistive part, i.e., the core of the film [modeled as R in the inset of Fig. 4(a)], forming an electric current. This entails that the drop of the electric field mostly takes place at the interface barrier, yielding the apparent high dielectric constant shown in Fig. 2(a) because of the apparent reduction of the dielectric thickness (measured capacitance is proportional to $1/d$).[9] On increasing temperature, the film resistivity decreases

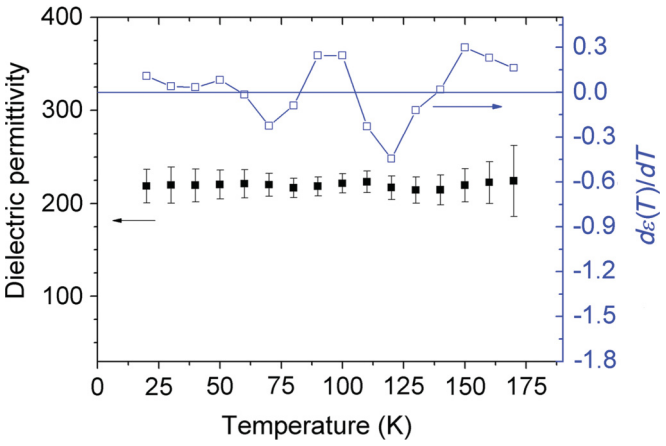

FIG. 5. (Color online) Temperature dependence of the intrinsic dielectric permittivity of BLNMO films obtained by impedance spectroscopy (left axis) and dielectric permittivity derivative (right axis).

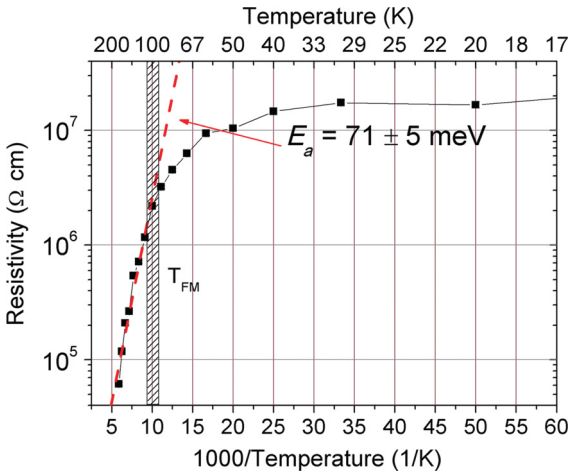

FIG. 6. (Color online) Temperature dependence of the resistivity of BLNMO films obtained by impedance spectroscopy. The dashed line shows the Arrhenius law fitting. The dashed region indicates the magnetic Curie temperature.

(and thus leakage σ_{dc} increases; Fig. 3), and charge carriers can respond to faster alternation of the electric field. Thus, the apparent enhancement of the dielectric constant due to the apparent reduction of the dielectric thickness is shifting toward higher frequencies on increasing temperature, consistent with the observed temperature evolution of data of Fig. 2(a). The cutoff frequency given by the frequency $\omega_{\max}$ at which losses ($\sim\varepsilon''$) show a peak [Fig. 2(b)] is given by the condition $\omega_{\max}(T) = [R(T) \cdot C]^{-1}$ (Ref. 9) and is therefore temperature dependent. Hence, it is reasonable to argue that the thermal activation of this apparent dielectric relaxation is driven by the temperature dependence of the resistivity, instead of the permanent dielectric dipoles suggested for LNMO films.[18] The dielectric relaxation of permanent dipole moments tends to occur at much higher frequencies, in the range of microwaves.[29]

From the fitting values of the R-CPE element (R, Q, and α), the intrinsic dielectric permittivity and the resistivity of BLNMO films can be obtained at each temperature, as shown in Figs. 5 and 6, respectively. The CPE exponent α, which decreases on increasing temperature [Fig. 4(d)], pointing to an enhanced nonideality of the dielectric behavior of BLNMO films upon heating, displays a defined anomaly ~100 K, closely coinciding with the ferromagnetic Curie temperature.

The dielectric permittivity of BLNMO films (Fig. 5) is found to be temperature independent, as expected for a ferroelectric material far below its ferroelectric transition temperature (~450 K[7]). The value of permittivity (~220) is in close agreement with the reported bulk value (~200).[3] In addition, around the magnetic ordering temperature T_{FM} (~100 K), there is no significant deviation of permittivity; however, the derivative of $d\varepsilon/dT$ shown in Fig. 5 (right axis) seems to indicate a subtle variation at a temperature close to the magnetic transition temperature, much like the anomaly at α (100 K) in Fig. 4(d), suggesting a possible small influence of the magnetic order and thus magnetoelectric response.

The temperature dependence of the resistivity $\rho(T)$ (Fig. 6) shows a semiconductorlike behavior, similar to what has been reported for other multiferroic perovskite oxides.[10] The resistivity decreases from $\sim 10^8$ Ω·cm at 20 K to $\sim 10^4$ Ω·cm at 170 K. The resistivity values obtained by impedance spectroscopy and σ_{dc} or, equivalently, the resistivity estimated by extrapolation of $\sigma'(\nu)$ from the plateau toward zero frequency (dashed lines in Fig. 3) are in good agreement, as shown by some illustrative values in Fig. 3 (inset). At temperatures above 100 K, the resistivity seems to behave thermally activated, following the Arrhenius law $\rho = \rho_0 \exp(E_a/k_B T)$ (dashed line in Fig. 6) with activation energy (71 ± 5 meV). Within the simplest picture, electron transport in BLNMO is related to electron hopping among a dissimilar electronic configuration of the B-cations, i.e., Ni^{2+} and Mn^{4+}. Not surprisingly, small activation energy was also reported for B-site-ordered double-perovskite LNMO thin films ($E_a \approx 32$ meV).[18] Hence, it is reasonable to suggest that multiferroic double-perovskite materials may suffer from a poorer insulating character with regard to their counterpart single perovskites. However, the observed activation energy is smaller than the predicted band gap in BNMO (~200–500 meV).[30,31]

A different behavior is found at lower temperatures ($T <$ 100 K). As shown in Fig. 6, in this temperature range, the resistivity deviates from the Arrhenius law, reflecting a change in the predominant conduction mechanism. An alternative conduction mechanism, such Mott's variable-range-hopping (VRH) or Efros and Shklovskii VRH conduction mechanisms—where $\rho = \rho_0 \exp(T_0/T^{1/\gamma})$, $\gamma = 4$ or 2—have been considered.[32–34] None of these models allow us to describe satisfactorily the whole temperature range. In any event, data in Fig. 6 suggest a change of either the transport mechanism or the relevant energy for activated transport occurring ~100 K. Interestingly, at this temperature, the film becomes ferromagnetic; thus, the magnetic order may have some influence on the conduction mechanism.

C. Magnetoelectric response

Figure 7(a) depicts the magnetocapacitance $MC(T) = [C(H) - C(0)]/C(0)$ of a Pt/BLNMO/Nb:STO system measured at 100 kHz at several temperatures. A high frequency was selected to minimize the contribution from interfaces to

the measured capacitance. At a given magnetic field, $MC(T)$ displays a nonmonotonic dependence on temperature. As shown in Fig. 7(b), $MC(T, 8\ \mathrm{T})$ attains a maximum (4.5% at 8 T) ~140 K. Data show a clear resemblance to $MC(T)$ ($\nu = 100$ kHz) reported for BNMO thin films.[19]

The maximum of the magnetocapacitance effect occurs at a temperature substantially above the ferromagnetic transition temperature (~100 K), where the largest magnetoelectric response, if any, is to be expected.[11] Moreover, the $\varepsilon'(\nu)$ and tan $\delta(\nu)$ data in Fig. 2 indicate that the temperature range in which $MC(T)$ shows the sharp increase coincides with the peak in ε'' and the step region in ε' at 100 kHz (marked with dashed line, Fig. 2) separating the two frequency regimes: the extrinsic low-frequency and the intrinsic high-frequency dielectric constant regimes. Indeed, for temperatures in which $\varepsilon'(\nu)$ is either in the low-frequency plateau or in the high-frequency plateau, $MC(H)$ is almost nonexistent. This suggests that the observed large MC effect may occur due to the shift of the steplike dielectric response because of the magnetic field-inducing change of film resistivity. As discussed in previous sections, in the step region of $\varepsilon'(\nu)$, small changes in the resistivity of BLNMO films may produce significant changes in the measured apparent dielectric permittivity; i.e., the positive MC effect shown in Fig. 7 might be due to the decrease of the resistivity of BLNMO films by applying a magnetic field.

We also performed magnetoimpedance spectroscopy (at $H = 0$ and 9 T) in a temperature range close to T_{FM} (80–130 K). Using the procedure explained in Sec. III B and fitting data by Eq. (2), the intrinsic BLNMO dielectric permittivity and resistivity can be obtained, with and without an applied magnetic field. Results are shown in Fig. 8. It is clear in Fig. 8(a) that, within the experimental resolution $\varepsilon(T, 9\ \mathrm{T})$ and $\varepsilon(T, 0\ \mathrm{T})$ are coincident. Moreover, the BLNMO resistivity is found to decrease upon increasing the magnetic field [Fig. 8(b)], a common feature in manganites, thus providing support to the preceding claim that the magnetocapacitance shown in Fig. 7 arises from the magnetoresistive character of BLNMO rather than from magnetoelectric coupling.

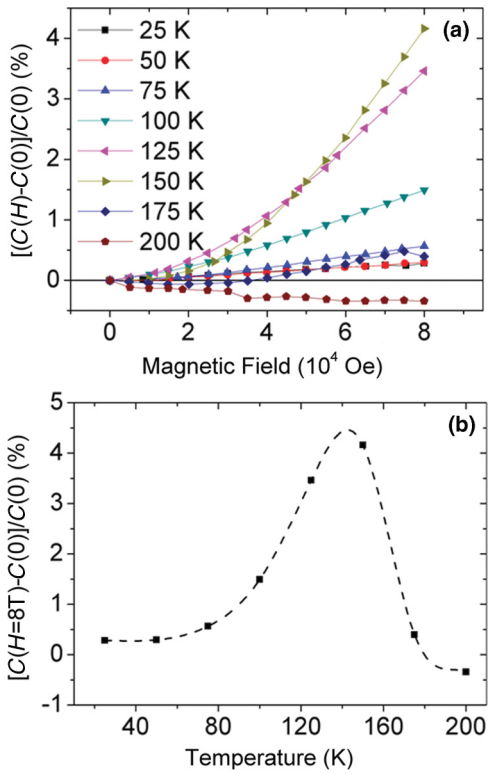

FIG. 7. (Color online) (a) Magnetocapacitance of a Pt/BLNMO/Nb:STO system measured at 100 kHz at different temperatures. (b) Temperature dependence of the magnetocapacitance of a Pt/BLNMO/Nb:STO system at $H = 8$ T and 100 kHz. The dashed line is a visual guide.

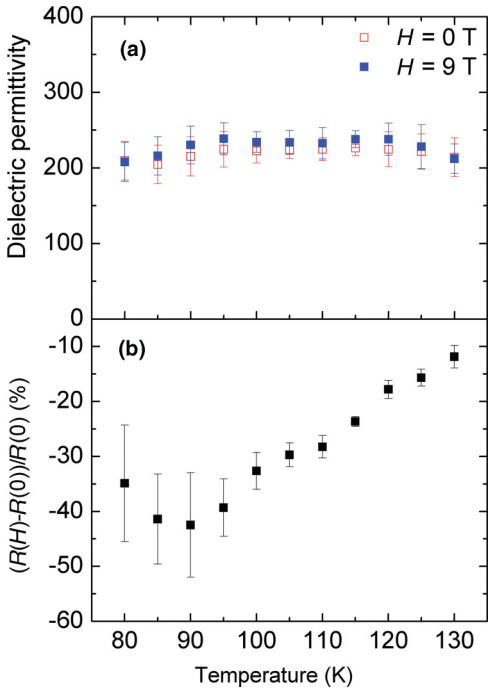

FIG. 8. (Color online) (a) Temperature dependence of the intrinsic dielectric permittivity of BLNMO films obtained by magnetoimpedance spectroscopy for $H = 0$ T (open symbols) and $H = 9$ T (solid symbols). (b) Magnetoresistance of BLNMO films obtained by magnetoimpedance spectroscopy (for $H = 0$ T and $H = 9$ T).

IV. CONCLUSION

We have thoroughly investigated the dielectric response of $(Bi_{0.9}La_{0.1})_2NiMnO_6$ thin films. Impedance spectroscopy technique has allowed us to prove that extrinsic contributions, such as interface capacitance, together with the temperature dependence of the resistivity of the films, can explain the apparent large enhancement of the dielectric constant at high temperatures and low frequency and the temperature dependence of the dielectric relaxation of BNMO films. We have shown, by appropriate selection of measuring conditions (frequency) and circuit analysis, that the intrinsic dielectric permittivity of BLNMO films have been extracted, obtaining a value close to the bulk one (~200), and that in the temperature range within which the material orders magnetically, the permittivity remains virtually constant. The electron conduction in BLNMO films, at least at high temperature, can be described by a thermally activated model, with an activation energy of ~70 meV, which is substantially lower than theoretical predictions of the band gap in these compounds. Finally, we

have shown that although the films display a sizable magnetocapacitance, this effect results from the magnetoresistance of BLNMO rather than from a genuine magnetoelectric effect, because the intrinsic dielectric permittivity was found to be independent of the magnetic field. These observations point to a weak coupling, if present, between the ferroelectric and the ferromagnetic order in $(Bi,La)_2NiMnO_6$ compounds.

ACKNOWLEDGMENTS

We thank C. J. M. Daumont for assistance in the dielectric measurements. Financial support by the Spanish government (Grants No. MAT2011-292691-C03, No. MAT2011-0292691-C01, and No. NANOSELECT CSD2007-00041) and by Generalitat de Catalunya (Grant No. 2009 SGR 0376) are acknowledged.

*eric.langenberg.perez@gmail.com

[1] R. Ramesh and N. Spaldin, Nat. Mater. **6**, 21 (2007).

[2] J. B. Goodenough, *Magnetism and the Chemical Bond* (R. E. Krieger Pub. Co., Huntington, NY, 1976).

[3] M. Azuma, K. Takata, T. Saito, S. Ishiwata, Y. Shimakawa, and M. Takano, J. Am. Chem. Soc. **127**, 8889 (2005).

[4] N. S. Rogado, J. Li, A. W. Sleight, and M. A. Subramanian, Adv. Mater. **17**, 2225 (2005).

[5] C.-H. Yang, S.-H. Lee, T. Y. Koo, and Y. H. Jeong, Phys. Rev. B **75**, 140104 (2007).

[6] Y. Kobayashi, M. Shiozawa, K. Sato, K. Abe, and K. Asai, J. Phys. Soc. Jpn. **77**, 084701 (2008).

[7] E. Langenberg, I. Fina, P. Gemeiner, B. Dkhil, L. Fàbrega, M. Varela, and J. Fontcuberta, Appl. Phys. Lett. **100**, 022902 (2012).

[8] E. Langenberg, J. Rebled, S. Estradé, C. J. M. Daumont, J. Ventura, L. E. Coy, M. C. Polo, M. V. García-Cuenca, C. Ferrater, B. Noheda, F. Peiró, M. Varela, and J. Fontcuberta, J. Appl. Phys. **108**, 123907 (2010).

[9] G. Catalan, Appl. Phys. Lett. **88**, 102902 (2006).

[10] R. Schmidt, J. Ventura, E. Langenberg, N. M. Nemes, C. Munera, M. Varela, M. García-Hernández, C. León, and J. Santamaría, Phys. Rev. B **86**, 035113 (2012).

[11] T. Kimura, S. Kawamoto, I. Yamada, M. Azuma, M. Takano, and Y. Tokura, Phys. Rev. B **67**, 180401(R) (2003).

[12] M. Li, D. C. Sinclair, and A. R. West, J. Appl. Phys. **109**, 084106 (2011).

[13] P. Lunkenheimer, V. Bobnar, A. V. Pronin, A. I. Ritus, A. A. Volkov, and A. Loidl, Phys. Rev. B **66**, 052105 (2002).

[14] L. He, J. B. Neaton, M. H. Cohen, D. Vanderbilt, and C. C. Homes, Phys. Rev. B **65**, 214112 (2002).

[15] D. O'Neill, R. M. Bowman, and J. M. Gregg, Appl. Phys. Lett. **77**, 1520 (2000).

[16] J. Yu, P. Paradis, T. Ishikawa, and S. Yoda, Appl. Phys. Lett. **85**, 2899 (2004).

[17] N. Biškup, A. de Andrés, J. L. Martinez, and C. Perca, Phys. Rev. B **72**, 024115 (2005).

[18] P. Padhan, H. Z. Guo, P. LeClair, and A. Gupta, Appl. Phys. Lett. **92**, 022909 (2008).

[19] P. Padhan, P. LeClair, A. Gupta, and G. Srinivasan, J. Phys. Condens. Matter **20**, 355003 (2008).

[20] J. T. S. Irvine, D. C. Sinclair, and A. R. West, Adv. Mater. **2**, 132 (1990).

[21] E. Langenberg, M. Varela, M. V. García-Cuenca, C. Ferrater, M. C. Polo, I. Fina, L. Fàbrega, F. Sánchez, and J. Fontcuberta, J. Magn. Magn. Mater. **321**, 1748 (2009).

[22] From top to top, electrode dielectric measurements entail measuring two identical capacitors of thickness d, which is the sample thickness, connected in series. Equivalently, it can be considered as measuring one unique capacitor of the thickness $2d$.

[23] M. Sakai, A. Masuno, D. Kan, M. Hashisaka, K. Takata, M. Azuma, M. Takano, and Y. Shimakawa, Appl. Phys. Lett. **90**, 072903 (2007).

[24] A. K. Jonscher, *Dielectric Relaxations in Solids* (Chelsea Dielectrics Press, London, 1983).

[25] J. R. Macdonald, *Impedance Spectroscopy* (Wiley, New York, 1987).

[26] F. D. Morrison, D. J. Jung, and J. F. Scott, J. Appl. Phys. **101**, 094112 (2007).

[27] R. Schmidt and A. W. Brinkman, J. Appl. Phys. **103**, 113710 (2008).

[28] F. Berkemeier, M. R. S. Abouzari, and G. Schmitz, Phys. Rev. B **76**, 024205 (2007).

[29] T. Tsurumi, J. Li, T. Hoshima, H. Kakemoto, M. Nakada, and J. Akedo, Appl. Phys. Lett. **91**, 182905 (2007).

[30] A. Ciucivara, B. R. Sahu, and L. Kleinman, Phys. Rev. B **76**, 064412 (2007).

[31] Y. Uratani, T. Shishidou, F. Ishii, and T. Oguchi, Phys. B **383**, 9 (2006).

[32] A. Seeger, P. Lunkenheimer, J. Hemberger, A. A. Mukhin, V. Y. Ivanov, A. M. Balbashov, and A. Loidl, J. Phys. Condens. Matter **11**, 3273 (1999).

[33] D. Yu, C. Wang, B. L. Wehrenberg, and P. Guyot-Sionnest, Phys. Rev. Lett. **92**, 216802 (2004).

[34] A. L. Efros and B. I. Shklovskii, J. Phys. C. Solid State Phys. **8**, L49 (1975).